

Ground state properties of a trapped few-Boson system under rotation —beyond the “lowest Landau level” approximation—

Xiaji Liu^{1,3}, Hui Hu¹, Lee Chang², and Shi-Qun Li^{1,3}

¹*Department of Physics, Tsinghua University, Beijing 100084, China*

²*Center for Advanced Study, Tsinghua University, Beijing 100084, China*

³*Key Laboratory for Quantum Information and Measurements Ministry of Education
and Center for Atomic and Molecular Nanosciences, Tsinghua University, Beijing 100084, China*

(November 12, 2018)

We consider a harmonically trapped few-Boson system under rotation and investigate the ground state properties beyond the usual “lowest Landau level” approximation by using exact diagonalizations in a restricted Hilbert subspace. We find that both the effective interaction energy and density distribution are strongly affected by the two-body interaction strength.

PACS numbers:03.75.Fi, 05.30.Jp, 67.40.Db, 67.40.Vs

Following the experimental realization of Bose-Einstein condensation of alkali-metal atoms [1], there has been much attention attached to the behavior of these systems under rotation both experimentally and theoretically. Matthews *et al.* [2] created vortices in a two-component system, and Madison *et al.* [3] studied the rotations in a stirred one-component Bose-Einstein condensate. Theoretical studies have mainly focused on the Thomas-Fermi regime of strong interactions [4–8] or on the limit of weak interactions between the atoms [9–15]. In the latter case, most research works have applied the “lowest Landau Level (LLL)” approximation, in which all the bosons are in single-particle orbitals with radial quantum number $n = 0$ and angular momentum m having the same sign as the total angular momentum. The intermediate regime of moderate interaction, however, is rarely concerned [16,17].

In this Brief Report, we would like to study ground state properties of a trapped rotating Bose-Einstein condensate with an *arbitrary* two-body interaction strength beyond the LLL approximation. To attack the problem, we calculate low-lying states of a few-Boson system by using the exact diagonalization method. We assume that our numerical computation is *qualitatively* applicable for a rotating Bose-Einstein condensate though the number of bosons is limited to a small value of $N = 16$. We also assume that the cloud of atoms rotates about some axis, and that the system is in its ground state with respect to this axis, which implies that our problem is essentially two dimensional.

The trapped Bose-Einstein condensate, comprised of N repulsively interacting alkali atoms with mass M and s-wave scattering length a_{sc} , obeys the many-body Hamiltonian

$$\mathcal{H} = \sum_{j=1}^N \left\{ -\frac{1}{2} \nabla_j^2 + \frac{1}{2} \mathbf{r}_j^2 \right\} + g \sum_{i < j} 2\pi \delta(\mathbf{r}_i - \mathbf{r}_j), \quad (1)$$

where the energy and length are given throughout in scaled harmonic oscillator units $\hbar\omega$ and $a = \sqrt{\hbar/M\omega}$, respectively. The two-body contact interaction strength is characterized by a dimensionless coupling constant

$g = a_{sc}/a$. As we shall see, the problem has three different interesting regimes parametrized by the product gN : the Thomas-Fermi regime $gN \gg 1$, the moderate interaction regime $gN \sim 1$, and the weak interaction regime $gN \ll 1$. To diagonalize the Hamiltonian, Eq. (1), the single-particle states of the Fock state are chosen to be eigenstates of the two-dimensional harmonic oscillator, i.e.,

$$\epsilon_{nm} = 2n + |m| + 1, \quad (2)$$

$$\psi_{nm} = \sqrt{\frac{n!}{\pi(n+|m|)!}} r^{|m|} e^{-\frac{r^2}{2}} L_n^{(|m|)}(r^2) e^{im\varphi}, \quad (3)$$

where $L_n^{(|m|)}(r^2)$ is the associated Laguerre polynomial. n and m are the radial and angular momentum quantum number, respectively. Previous studies in weak interaction limit usually take single particle states with $n = 0$ and $m = 0, +1, +2, +3, \dots$, which corresponds to the LLL approximation. Here we set up Fock states by extending to $n \leq 2$ and $-2 \leq m \leq 4$ [18], and sample over the full Hilbert space with a fixed number of bosons. From this sampling, only those Fock states with a given total orbital angular momentum L and a configuration energy (corresponding to the sum of occupied single particle energies) less than or equal to a specified cutoff energy E_c are included (see figure 1 below for example). The purpose was to select only the most important Fock states from the full basis, thereby reducing the matrix dimension to an acceptable size $d \lesssim 10^5$. Once the active Fock states are constructed, we calculate the matrix elements and subsequently diagonalize the matrix by using the Davidson algorithm [19], which is very efficient to solve the eigenvalue problem with a large and sparse matrix.

It is important to point out that the above diagonalization scheme only in principle yields an exact solution of the many-body problem. For reasons of numerical feasibility it is necessary to truncate the set of basis functions to be used in the diagonalization. One then has to make sure that convergence of the ground state energy is reached with respect to the cutoff. As the required matrix size increases rapidly with gN and L , computational expenses severely restrict the calculations to only

the smallest systems at not too large values of g . Thus, with increasing boson number or g , the results become less accurate due to the restricted number of basis states that can be included in the calculations. Figure 1 shows the convergence of the ground state energy as a function of the cutoff energy E_c for a system of $N = 10$ bosons at $L = 10$. The lowest possible Fock state has all ten bosons distributed in the lowest Landau level, and the corresponding configuration energy equals to $N + L = 20$. This means that for the ground state energy with different cutoff energies displayed in figure 1 all excitations up to an energy $E_c - 20$ are included. It is readily seen that both the case with a moderate interaction strength $gN = 1$ (figure 1a) and a relatively strong interaction strength $gN = 3$ (figure 1b) show convergence at $E_c > 30$. The smaller g is, the more rapidly the convergence reaches. Therefore, we conclude that our numerical results shown below is very accurate for a weak or moderate interaction strength, and also qualitatively accurate in the relatively strong interaction regime. In what follows, we take $E_c = N + L + 10$.

We now analyze the influence of interaction strength g on ground state energies as a function of the total angular momentum, which may be written as

$$E_{gs}(L) = (N + L) + gV_{int,L}, \quad (4)$$

where $V_{int,L}$ is introduced as a *scaled* effective interaction energy. Figure 2 shows the L dependence of $V_{int,L}$ of a system of $N = 16$ bosons for $g = 0.006, 0.1$ and 0.3 . For comparison, the result with LLL approximation is also displayed. Note that the case of $g = 0.006$ is closer to experimental values for ^{87}Rb [20], i.e., $a_{sc} \sim 100a_0 = 5.29$ nm and $a = 1.25 \times 10^{-4}$ cm. For all three interaction strengths, the interaction energy $V_{int,L}$ simply decreases linearly or near linearly with increasing the angular momentum. At $N = L$, a kink appears in slope. This is a hint of condensation into a vortex state: in macroscopic superfluids, the state for $L = N$ would have a condensate of unit angular momentum and would be lower in energy than neighboring ground states. In the weak interaction limit ($gN = 0.096 \ll 1$), our results only show slightly deviation from that with LLL approximation. However, with increasing the interaction strength, the interaction energy $V_{int,L}$ drops significantly for each angular momentum. This implies a spatial reconfiguration of bosons since they should push away from each other to reduce the strong interaction as g increases.

We next investigate the density distribution of bosons for various interaction strengths as shown in figure 3. In general, the density is found to become decreasingly small and broad as g increases. For all angular momenta, the shape of curves for the weak and relatively strong interaction strength differs largely: not only the maximum density of the former case is nearly two times larger than that of the latter one, but the maximum position is also shifted strongly. Moreover, when the angular momentum is closer to $L = N$, a maximum surrounded by an out

ring of lower density appears at the $r = 0$ for a relatively strong interaction strength $g = 0.3$ (see figure 3c).

To further examine the structure of the ground state, we calculate the conditional probability distributions (CPDs), which measure the density correlation among bosons [21]. Unlike the usual density distribution, which is *circularly symmetric* under the rotation invariant confinement, the CPD reflects an *intrinsic* density distribution of bosons [22]. And thus it is indeed an observable quantity in experiments instead of the circularly symmetric density distribution. This is best illustrated for a condensed boson gas, where the circularly symmetry is broken spontaneously, and CPD is then related to the measurement of boson density [22]. Note also that the CPD has been extensively used in the study of electron correlations in doubly excited helium-like atoms [23] and analysis of the formation of Wigner molecule in quantum dots [24]. We define the CPD for finding one boson at \mathbf{r} given that another is at \mathbf{r}_0 as

$$\mathcal{P}(\mathbf{r} | \mathbf{r}_0) = \frac{\langle \Psi_{GS} | \sum_{i \neq j} \delta(\mathbf{r} - \mathbf{r}_i) \delta(\mathbf{r}_0 - \mathbf{r}_j) | \Psi_{GS} \rangle}{(N-1) \langle \Psi_{GS} | \sum_j \delta(\mathbf{r}_0 - \mathbf{r}_j) | \Psi_{GS} \rangle}, \quad (5)$$

where $|\Psi_{GS}\rangle$ represents the ground state. In figure 4, we show a plot of CPDs for some selected angular momenta and for a system of $N = 16$ bosons. With increasing the two-body interaction strength, the bosons spread more widely in x-y plane as expected, in line with density distributions shown in figure 3. On the other hand, the evolution of producing a single vortex state at $N = L$ does not change significantly even as g is varied over several (~ 2) orders of magnitude.

In conclusion, we have studied the ground state of a repulsively interacting Bose-Einstein condensate with a nonvanishing angular momentum. We found that all physical quantities, especially the effective interaction energy, are strongly affected by a dimensionless interaction strength g . We realize that our result is based on a few-Boson system, and its validity to a Bose-Einstein condensate should be further checked by more rigorous analytic and numerical treatments, such as the quantum Monte-Carlo simulation. We also note that although the so-far published experiments have mainly studied systems that do not satisfy the condition $gN \sim 1$ or $gN \ll 1$, systems that do satisfy this condition are accessible with current experimental techniques [25].

We would like to thank Y. Zhou and Y.-X. Miao for their stimulating discussions. X. Liu was supported by NSF-China (Grant No. 19975027 and 19834060). H. Hu acknowledges the support of Profs. Jia-Lin Zhu and Jia-Jiong Xiong, and a research grant from NSF-China (Grant No. 19974019).

- [1] F. Dalfovo, S. Giorgini, L. P. Pitaevskii, and S. Stringari, *Rev. Mod. Phys.* **71**, 463 (1999).
- [2] M. R. Matthews, B. P. Anderson, P. C. Haljan, D. S. Hall, C. E. Wieman, and E. A. Cornell, *Phys. Rev. Lett.* **83**, 2498 (1999).
- [3] K. W. Madison, F. Chevy, W. Wohlleben, and J. Dalibard, *Phys. Rev. Lett.* **84**, 806 (2000); F. Chevy, K. W. Madison, and J. Dalibard, *Phys. Rev. Lett.* **85**, 2223 (2000); K. W. Madison, F. Chevy, W. Wohlleben, and J. Dalibard, e-print cond-mat/0004037 (2000).
- [4] D. Rokhsar, *Phys. Rev. Lett.* **79**, 2164 (1997).
- [5] S. Sinha, *Phys. Rev. A* **55**, 4325 (1997).
- [6] D. L. Feder, C. W. Clark and B. I. Schneider, *Phys. Rev. Lett.* **82**, 4956 (1999).
- [7] A. A. Svidzinsky and A. L. Fetter, *Phys. Rev. Lett.* **84**, 5919 (2000).
- [8] K.-P. Marzlin, W. Zhang, and B. C. Sanders, *Phys. Rev. A* **62**, 013602 (2000).
- [9] N. K. Wilkin, J. M. F. Gunn, and R. A. Smith, *Phys. Rev. Lett.* **80**, 2265 (1998).
- [10] R. A. Butts and D. S. Rokhsar, *Nature* **397**, 327 (1999). G. M. Kavoulakis, B. Mottelson, and C. J. Pethick, *Phys. Rev. A* **62**, 063605 (2000).
- [11] B. Mottelson, *Phys. Rev. Lett.* **83**, 2695 (1999).
- [12] G. F. Bertsch and T. Papenbrock, *Phys. Rev. Lett.* **83**, 5412 (1999); T. Papenbrock and G. F. Bertsch, *Phys. Rev. A* **63**, 023616 (2001).
- [13] N. K. Wilkin and J. M. F. Gunn, *Phys. Rev. Lett.* **84**, 6 (2000). N. R. Cooper and N. K. Wilkin, *Phys. Rev. B* **60**, 16279 (1999).
- [14] A. D. Jackson, G. M. Kavoulakis, B. Mottelson, and S. M. Reimann, *Phys. Rev. Lett.* **86**, 945 (2001).
- [15] A. D. Jackson and G. M. Kavoulakis, *Phys. Rev. Lett.* **85**, 2854 (2000). R. A. Smith and N. K. Wilkin, *Phys. Rev. A* **62**, 061602 (2000). T. Papenbrock and G. F. Bertsch, e-print cond-mat/0008286 (2000). Wen-Jui Huang, *Phys. Rev. A* **63**, 015602 (2001).
- [16] M. A. H. Ahsan and N. Kumar, e-print cond-mat/0011212 (2000).
- [17] T. Isoshima and K. Machida, *J. Phys. Soc. Jpn.* **68**, 487 (1999).
- [18] We have checked numerically that the precision of our results is only slightly improved by including more single particle states.
- [19] E. R. Davidson, *J. Comput. Phys.* **17**, 87 (1975). A. Stathopoulos and C.F. Fischer, *Comput. Phys. Commun.* **79**, 268 (1994).
- [20] P. S. Julienne, F. H. Mies, E. Tiesinga, and C. J. Williams, *Phys. Rev. Lett.* **78**, 1880 (1997).
- [21] X. Liu, H. Hu, L. Chang, W. Zhang, S.-Q. Li, and Y.-Z. Wang, e-print cond-mat/0012259, to appear in *Phys. Rev. Lett.* (2001).
- [22] The difference between CPD and usual boson density can be naturally interpreted as follows: the CPD describes bosons in their *intrinsic (body-fixed)* frame of the reference, while the density distribution describes bosons in the laboratory frame of reference where the rotational and center-of-mass displacements are superimposed upon the intrinsic probability density. However, in the mean-field treatment (under an assumption of spontaneous

symmetry breaking), the many-body condensate wavefunction is taken to be the product of the single-particle state $\Psi_{GS}(\mathbf{r}_1, \mathbf{r}_2, \dots, \mathbf{r}_N) = \prod_{i=1}^N \psi(\mathbf{r}_i)$, and the corresponding CPD is simply reduced to the density distribution of bosons $\mathcal{P}(\mathbf{r} | \mathbf{r}_0) = |\psi(\mathbf{r})|^2$.

- [23] G. S. Ezra and R. S. Berry, *Phys. Rev. A* **28**, 1974 (1983); see also R. S. Berry in *Structure and Dynamics of Atoms and Molecules: Conceptual Trends*, edited by J. L. Calais and E. S. Kryachko (Kluwer, Dordrecht, 1995) p. 155, and references therein.
- [24] C. Yannouleas and U. Landman, *Phys. Rev. Lett.* **85**, 1726 (2000); *Phys. Rev. B* **61**, 15895 (2000).
- [25] S. Inouye, M. R. Andrews, J. Stenger, H.-J. Miesner, D. M. Stamper-Kurn, and W. Ketterle, *Nature* **392**, 151 (1998).

Figures Captions

Fig.1. Ground state energy of a single vortex state versus the cutoff energy for a system of $N = 10$ bosons at the moderate (a) and relatively strong (b) interaction strengths. The energy is measured in units of $\hbar\omega$. Both the two cases show convergence at $E_c > N + L + 10$.

Fig.2. $V_{int,L}$ (in units of $\hbar\omega$) as a function of angular momentum for different two-body interaction strength. In the LLL approximation, it is described precisely by an algebraic expression $V_{int,L} = N(N - L/2 - 1)$ for $2 \leq L \leq N$ [12,15].

Fig.3. Density distribution of $N = 16$ bosons for various angular momenta. The unit of length is the oscillator length $a = \sqrt{\hbar/M\omega}$. The short dashed, dotted, dash dotted lines correspond to $g = 0.006, 0.1$, and 0.3 , respectively. The results with LLL approximation is also delineated by a solid line for comparison.

Fig.4. Selected conditional probability distributions for a system of $N = 16$ bosons. The value of x, y in each subplot ranges from $-3.0a$ to $+3.0a$. $\mathbf{r}_0 = (0, 1.0a)$, and other choice of \mathbf{r}_0 does not alter our results qualitatively.

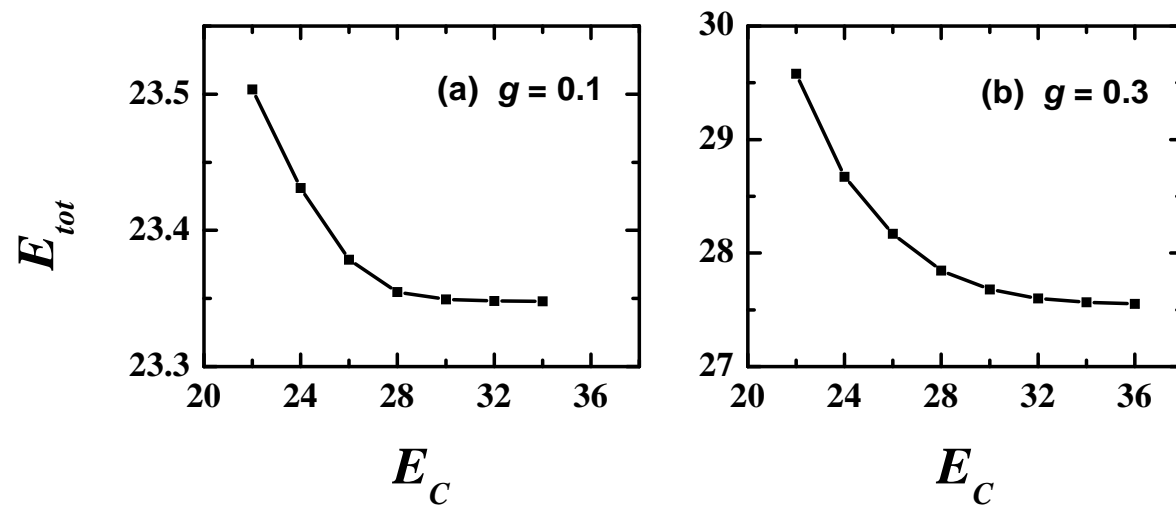


Fig. 1
Ground state properties of a trapped
X. Liu *et al.*

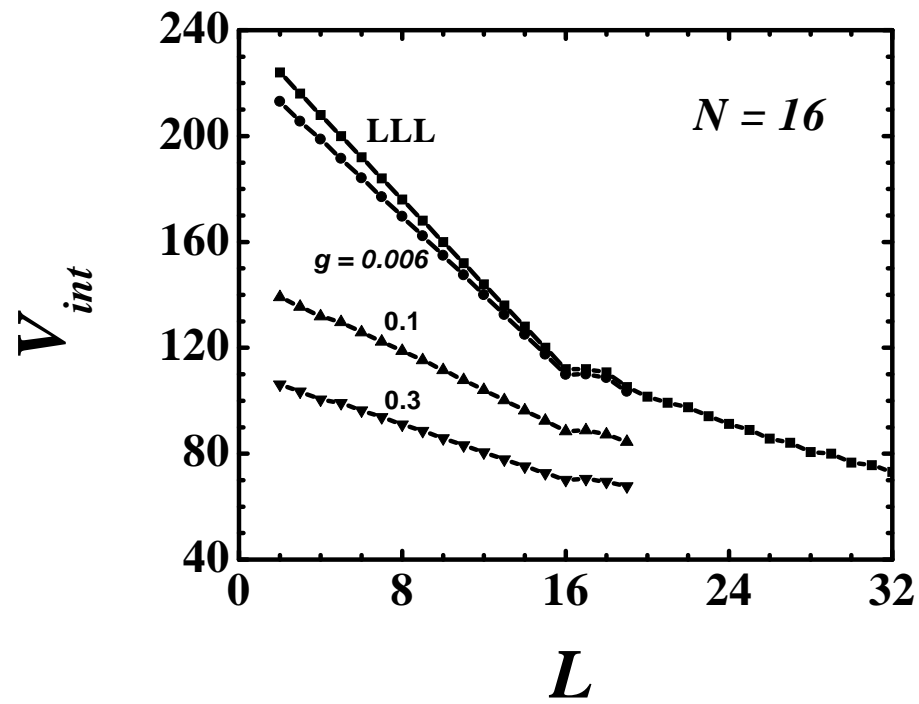


Fig. 2
 Ground state properties of a trapped
 X. Liu *et al.*

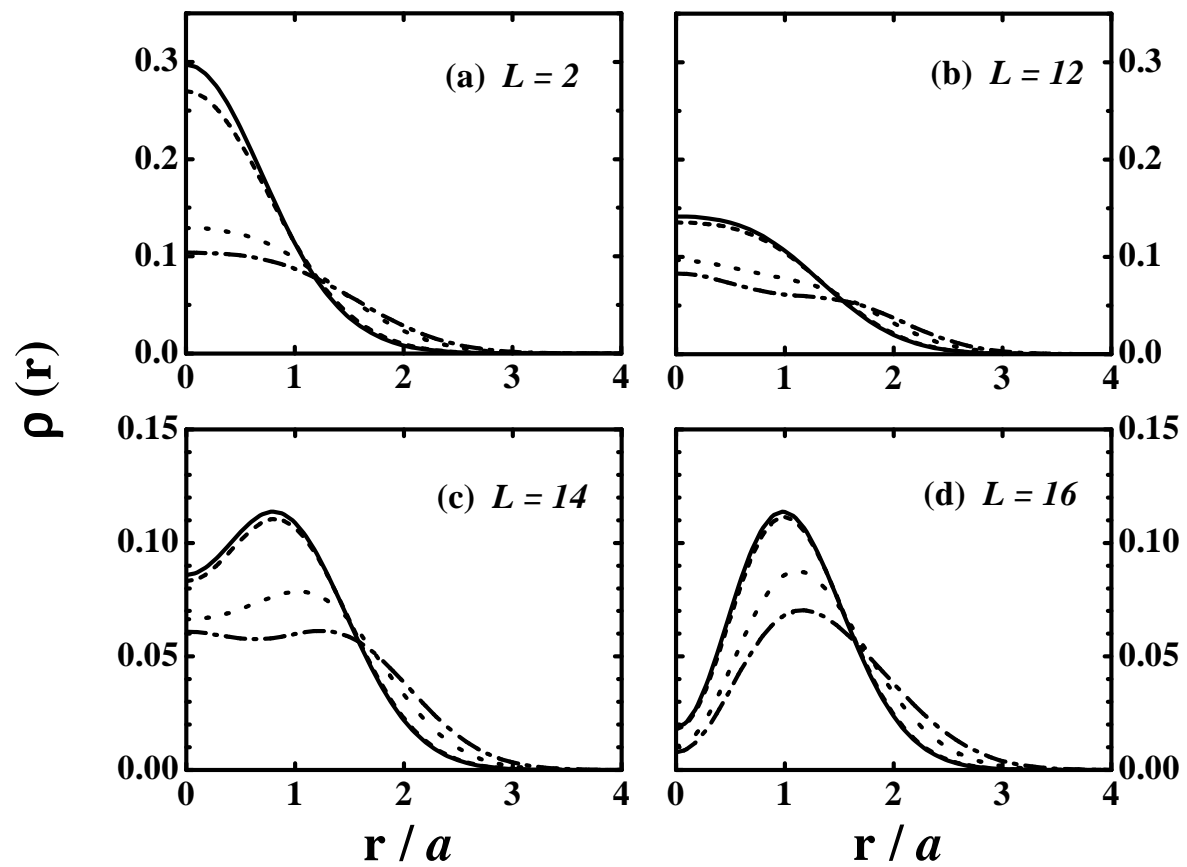


Fig. 3
Ground state properties of a trapped
X. Liu *et al.*